Free Energy Perturbation and Molecular Dynamics Studies of [1_6]Starand with Various Alkali Metal Ions

Seung Joo Cho and Peter A. Kollman*

Department of Pharmaceutical Chemistry, University of California at San Francisco, San Francisco, California 94143

Received December 2, 1998

Strong affinity and high selectivity are desirable characteristics of hosts in host−guest chemistry. Because starands exhibit high rigidity and sphericity, one would expect them to have interesting properties. We have investigated and predicted the complexation behavior of [1_6]starand with various alkali metal ions, using free energy perturbation and molecular dynamics methods. Our calculated geometries and energetics with the AMBER force field agree with previous ab initio results; energy minimization also predicts that the Li^+ binds not at the center but on the outside of the cavity. Additionally, we have calculated the binding free energy differences for various alkali metal ions. The results from the gas phase simulations show that the binding free energy difference decreases as the radius increases, with only a small difference between the binding enthalpy difference and binding free energy difference. This small entropy effect in the gas phase is likely due to the structural rigidity of starand and the strong cation−ligand interactions. When the complexes lie immersed in water, the order of binding free energies reverses, i.e., the binding energy increases as the ionic radius increases. This reversal of order is thus due to the solvent effect. To investigate why water favors complexation with larger ions, we performed radial distribution function (RDF) analyses from alkali ions to water oxygens. Water coordination numbers for the free solvated ions and for those in complexes were obtained from the RDF data. The relative free energy of binding seems to be related to the solvation energy of alkali metal ions. We have also calculated the absolute binding free energies of Rb^+ and Cs^+ in water. Notwithstanding our expectation from the appearance of this host, these calculations predict that the alkali metals do not bind strongly to [1_6]starand in water. These results further demonstrate the important contribution of hydration in host−guest chemistry.

Introduction

The scientific and practical interest in ionophores as complexing agents for cations is extensive.[1] Since the discovery of crown ether ionophores, diverse hosts have been extensively investigated for desirable functionalities.[2] As a result, it is well-established that host−guest size complementarity plays a very crucial role in determining both affinity and selectivity in host−guest chemistry.[3] Another important factor in host−guest chemistry has also became clear, during this intense research of diverse hosts, but is less appreciated. Host rigidity also plays an important role in affinity and selectivity.[4]

Free energy perturbation (FEP) methods combined with molecular dynamics (MD) or Monte Carlo (MC) have successfully provided a better understanding of relatively small synthetic hosts. These theoretical calculations usually agree with experiments, having reproduced the experimentally observed host−guest size complementarity.[5,6] Moreover, these calculations often provided valuable insights that could often explain the detailed molecular structural knowledge of host and/or solvent. Sun et al. managed to estimate the macrocyclic effect on the experimental binding free energy difference of 18-crown-6 and its linear analogue.[7] Miyamoto et al. calculated relative free energies of cation binding to a calixspherand.[8] They found that the experimental preference for K^+ derives from the solvation structure in water. Analogously, Mazor et al. realized that the solvation

* To whom correspondence should be addressed. Tel: (415) 476-4763. Fax: (415) 476-0688. E-mail: pak@cgl.ucsf.edu.

(1) (a) *Host−Guest Complex Chemistry: Macrocycles*; Vögtle, F.; Weber, E. Springer-Verlag: Berlin, Heildelberg, New York, 1985. (b) *Host−Guest Complex Chemistry I, II, III*; Vögtle, F., Ed.; Springer-Verlag: Berlin, Heildelberg, New York, Tokyo, 1981, 1982, 1984. (c) Jencks, W. P. *Acc. Chem. Res.* **1980**, *13*, 161. (d) McClelland R. A.; Santry, L. J. *Acc. Chem. Res.* **1979**, *16*, 394.

(2) (a) Plenio, H.; Diodone, R. *J. Am. Chem. Soc.* **1996**, *118*, 356. (b) Zhang, X. X.; Bordunov, A. V.; Bradshaw, J. S.; Dally N. K.; Kou, X.; Izatt, R. M. *J. Am. Chem. Soc.* **1995**, *117*, 11507. (c) Pedersen, C. J. *Science* **1988**, *241*, 536. (d) Cram, D. J. *Science* **1983**, *219*, 1177. (e) Lehn, J.-M. *Acc. Chem. Res.* **1978**, *11*, 49. (f) Dougherty, D. A.; Stauffer, D. A. *Science* **1990**, *250*, 1558.

(3) Steitwieser, A. Jr.; Heathcock, C. H. *Introduction to Organic Chemistry*, 3rd ed.; Macmillan: New York, 1985; pp 221−224.

(4) (a) Choi, H. S.; Suh, S. B.; Cho, S. J.; Kim, K. S. *Proc. Natl. Acad. Sci. U.S.A.* **1998**, *95*, 12094. (b) Kobuke, Y.; Kokubo, K.; Munakata, M. *J. Am. Chem. Soc.* **1995**, *117*, 12751. (c) Cram, D. J. *Angew. Chem., Int. Ed. Engl.* **1986**, *25*, 1039.

(5) (a) Mazor, M. H.; McCammon, J. A.; Lybrand, T. P. *J. Am. Chem. Soc.* **1990**, *112*, 4411. (b) Mazor, M. H.; McCammon, J. A.; Lybrand, T. P. *J. Am. Chem. Soc.* **1989**, *111*, 55. (c) Lybrand, T. P.; McCammon, J. A.; Wipff, G. *Proc. Natl. Acad. Sci. U.S.A.* **1986**, *83*, 833. (d) Auffinger, P.; Wipff, G. *J. Chim. Phys.-Chim. Biol.* **1991**, *88*, 2443. (e) Guilbaud, P.; Varnek, A.; Wipff, G. *J. Am. Chem. Soc.* **1993**, *115*, 8298. (f) Maye, P. V.; Venanzi, C. A. *J. Comput. Chem.* **1991**, *12*, 994. (g) Grootenhuis, P. D.; Kollman, P. A. *J. Am. Chem. Soc.* **1989**, *111*, 55.

(6) (a) Jorgensen, W. L.; Maxwell, D. S.; Tirado-Rives, J. *J. Am. Chem. Soc.* **1996**, *118*, 11225. (b) Jorgensen, W. L.; Nguyen, T. B. *Proc. Natl. Acad. Sci. U.S.A.* **1993**, *90*, 1194. (c) Jorgensen, W. L.; Nguyen, T. B.; Chao, I.; Houk, K. N.; Diederich, F. *J. Am. Chem. Soc.* **1992**, *114*, 114. (d) Jorgensen, W. L.; Boudon, S.; Nguyen, T. B. *J. Am. Chem. Soc.* **1989**, *111*, 755. (e) Jorgensen, W. L.; Briggs, J. M. *J. Am. Chem. Soc.* **1989**, *111*, 4190.

(7) (a) Sun, Y.; Kollman, P. A. *J. Am. Chem. Soc.* **1995**, *117*, 3599. (b) Dearden, D. V.; Dejsupa, C. Liang, Y.; Bradshaw, J. S.; Izatt R. M. *J. Am. Chem. Soc.* **1997**, *119*, 353. (c) Maleknia, S.; Brodbelt, J. *J. Am. Chem. Soc.* **1993**, *115*, 2837.

(8) Miyamoto, S.; Kollman, P. A. *J. Am. Chem. Soc.* **1992**, *114*, 3668.

10.1021/jo982367g CCC: $18.00
Published on Web 07/16/1999

structure of cations with 18-crown-6 in methanol provided a rationale for its preference.[5a]

Starands and spherands are structurally very similar, both being very rigid ionophores with well-defined spherical cavities, each comprised of oxygens with alternating up and down orientations, and two openings, one at the top and the other at the bottom. There have been many studies involving spherands, both theoretical and experimental. Empirically, spherands show very strong affinity and selectivity. A certain eight-subunit spherand shows a unique double preference toward alkali metals. These experimental data were reproduced and elucidated as a compromise between solvent effects and host−guest size complementarity.[9]

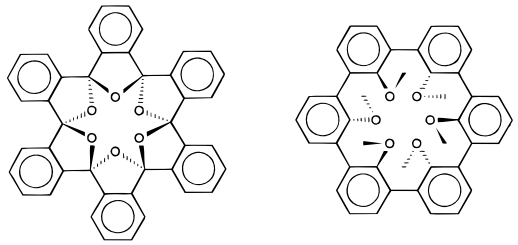

[1_6]Starand is one of the most preorganized ionophores, in that it contains no single bonds able to rotate. In this regard, [1_6]starand is expected to have unique properties.[10] Although there are some ab initio results[11] for this ionophore, no experimental data exists regarding the free energy differences of binding with respect to various alkali ions. Therefore, it is our goal to investigate the relative binding free energy of [1_6]starand toward alkali metal ions using FEP and MD.

Methods

All calculations were carried out with the AMBER 4.1[12] molecular dynamics package with the exception of the radial distribution function (RDF) data, which were obtained with a modified version of MINMD. The effective two-body parameters for the bond, angle, and dihedral angle terms are from Cornell et al.[13] Alkali ion parameters are from Aqvist,[14] and atomic charges were obtained by the two-stage RESP method.[15] Because [1_6]starand is rather large, the system as a whole was not studied by the Hartree−Fock (HF) method with the standard 6-31G* basis set. Fortunately, the cyclic hexamer [1_6]starand consists of a single repeating unit, and thus charge derivation for the monomer subunits alone, as shown in Figure 1, could be done using Gaussian 94.[16]

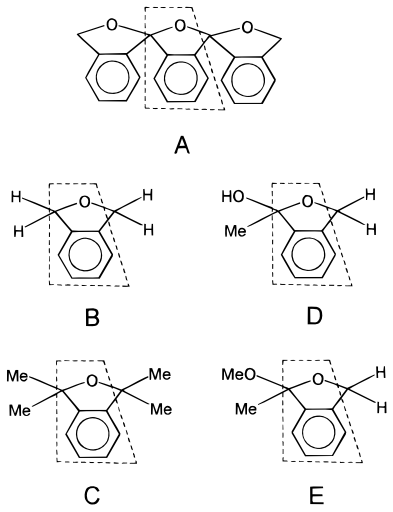

Figure 1. Various structures used in RESP charge calculations. The repeating units are denoted within dashed lines.

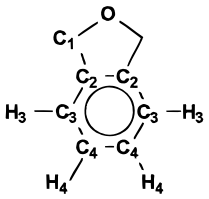

Figure 2. The 12 independent atoms of the repeating subunit in starand.

On a single fragment (enclosed by dashed lines in Figure 1) we calculated charges according to the labeling in Figure 2. In Figure 1, **A** is a trimer of repeating monomer subunits. **B**, **C**, **D**, and **E** are structures similar to the [1_6]starand subunit that exist as individual complete molecules, with only hydrogens (**B**) or methyl groups (**C**), or containing oxygen atoms as well (**D** and **E**). As discussed earlier in this paragraph, the charges obtained from fragment **A** should sufficiently and accurately represent each of the repeating subunits. Table 1 contains results that support this contention. Individual charges do not show much dependence on the choice of fragment. The biggest difference is in the C2 charge among fragments **A** and **B**, which is only about 0.1. Thus, atomic charges obtained for fragment **A** show relatively little sensitivity to atoms outside the fragment itself, thereby suggesting that the use of fragment **A** is an adequate procedure for charge derivation for the [1_6]starand. One other trend in Table 1 may also prove useful in utilizing this method of monomer charge derivation. The two fragments with additional oxygen atoms (**D** and **E**) have overall standard deviations significantly smaller than the two fragments without additional oxygen atoms (**B** and **C**). Therefore, when

(9) (a) Bayly C. I.; Kollman, P. A. *J. Am. Chem. Soc.* **1994**, *116*, 697. (b) Thomas, B. E.; Kollman, P. A. *J. Am. Chem. Soc.* **1994**, *116*, 3449.

(10) (a) Cho, S. J.; Hwang, H. S.; Park, J. M.; Oh, K. S.; Kim, K. S. *J. Am. Chem. Soc.* **1996**, *118*, 485. (b) Lee, W. Y.; Park, C. H. *J. Org. Chem.* **1993**, *58*, 7149. (c) Lee, W. Y.; Park, C. H.; Kim, H-.J. *J. Org. Chem.* **1994**, *59*, 878. (d) Lee, W. Y. *Synlett* **1994**, *10*, 765.

(11) Cui, C.; Cho, S. J.; Kim, K. S. *J. Phys. Chem. A* **1998**, *112*, 1119.

(12) (a) Pearlman, D. A.; Case, D. A.; Caldwell, J. W.; Ross, W. S. Cheatham, T. E.; Ferguson, D. M.; Seibel, G. L.; Singh, U. C.; Weiner, P.; Kollman, P. A. *AMBER 4.1*; University of California: San Francisco, 1991.

(13) Cornell, W. D.; Cieplak, P.; Bayly, C. I.; Gould, I. R.; Merz, J. M.; Ferguson, D. M.; Spellmeyer, D. C.; Fox, T.; Caldwell, J. W.; Kollman, P. A. *J. Am. Chem. Soc.* **1995**, *117*, 5179.

(14) Aqvist, J. *J. Phys. Chem.* **1990**, *94*, 8021.

(15) (a) Cornell, W. D.; Cieplak, P.; Bayly, C. I.; Kollman, P. A. *J. Am. Chem. Soc.* **1993**, *115*, 9620. (b) Cieplak, P.; Cornell, W. D.; Bayly, C.; Kollman, P. A. *J. Comput. Chem.* **1995**, *16*, 1357. (c) Bayly, C.; Cieplak, P.; Cornell, W. D.; Kollman, P. A. *J. Phys. Chem.* **1993**, *97*, 10269.

(16) Frisch, M. J.; Tricks, G. W.; Schlegel, H. B.; Gill, P. M. W.; Johnson, B. G.; Robb, M. A.; Cheeseman, J. R.; Keith, T. A.; Petersson, G. A.; Montgomery, J. A.; Raghavachri, K.; Al-Laham, M. A.; Zakrzewski, V. G.; Oritz, J. A.; Forseman, J. B.; Cioslowski, J.; Stefanov, B. B.; Nanayakara, A.; Challacombe, M.; Peng, C. Y.; Ayala, P. Y.; Chen, W.; Wong, M. W.; Andres, J. L.; Replogle, E. S.; Gomperts, R.; Martin, R. L.; Fox, D. J.; Binkely, J. S.; Defrees, D. J.; Baker, J.; Stewart, J. P.; Head-Gordon, M.; Gonzalez, C.; Pople, J. A. *Gaussian 94 Rev. A.1*; Gaussian Inc.: Pittsburgh, PA, 1995.

Table 1. Comparison of Charges Obtained from Different Fragments Shown in Figure 1[a]

	A	**B**	Δq_{AB}	C	Δq_{AC}	**D**	Δq_{AD}	**E**	Δq_{AE}
O	−0.415	−0.429	0.014	−0.394	−0.021	−0.459	0.044	−0.387	−0.028
C_1	0.455	0.406	0.049	0.377	0.078	0.490	−0.035	0.364	0.091
C_2	0.010	0.116	−0.105	0.077	−0.067	0.034	−0.023	0.052	−0.042
C_3	−0.200	−0.274	0.074	−0.233	0.033	−0.207	0.007	−0.186	−0.014
H_3	0.160	0.169	−0.009	0.173	−0.013	0.152	0.008	0.152	0.009
C_4	−0.133	−0.155	0.022	−0.158	0.024	−0.135	0.001	−0.152	0.018
H_4	0.142	0.156	−0.014	0.149	−0.006	0.140	0.003	0.146	−0.003
σ			0.058		0.042		0.020		0.035

[a] σ is the standard deviation of charge differences with respected to the charges obtained from fragment **A**. $\Delta q_{AB} = q_A - q_B$.

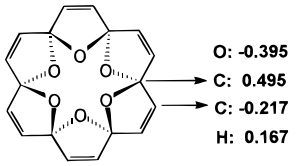

Figure 3. Model system of [1$_6$]starand and charges obtained by RESP.

Table 2. Geometries by X-ray, ab initio, and MM[a]

	[1$_6$]starand			model	
	X-ray[b]	3-21G[c]	MM	6-31+G*[d]	MM
O distances from mean plane[e]	0.80	0.79	0.83	0.77	0.84
O−O(para)[f]	3.82	3.86	3.77	3.77	3.76
O−O(ortho)	2.36	2.37	2.37	2.31	2.34
O−O(meta)	3.05	3.05	2.94	2.98	2.95

[a] Distances are in Å. [b] Reference 10d. [c] Reference 10a. [d] Reference 11. [e] Defined by the six innermost carbons. [f] O−O distance for opposing oxygens; like the para position in benzene. Ortho and meta positions are defined analogously.

obtaining the atomic charges within the fragment, one might reasonably include electronegative atoms adjacent to the fragment for the purpose of deriving charges with a lower variance.

Figure 3 displays a model starand system. This system was small enough to allow us to derive charges for this system as a whole, using the two-stage RESP method, by the 6-31G* Hartree−Fock method at the AM1 optimized geometry. The geometry of this optimized structure was very similar to the 6-31+G* optimized structure. The charges of the model starand system are also shown in Figure 3.

The [1$_6$]starand system was built on the basis of the highly symmetric D_{3d} X-ray structure, and the model starand system was built on the basis of the highly symmetric D_{3d} ab initio (HF) structure. These structures were then optimized using the force field described above. Because the systems are very rigid and there is no single bond to rotate, the structures from X-ray, ab initio, and molecular mechanics are essentially the same for both [1$_6$]starand and model starand. For [1$_6$]starand, the distances from the center of mass to oxygen are 1.909 Å from X-ray, 1.929 Å from ab initio (3-21G), and 1.887 Å from the molecular mechanics minimized structure. For the model system, the distances are 1.884 Å from ab initio (HF/6-31+G*) and 1.882 Å from the molecular mechanics minimized structure. The structural data are listed in Table 2.

To compare with previous ab initio results (MP2/6-31+G*//HF/6-31+G*), the binding energies are calculated in both binding modes, one in which ions attach to the cavity on the outer surface and the other where ions reside at the center of the host. The binding energies are listed in Table 3.

Table 3. Binding Energies of the Starand and Model Complexes[a]

		Li^+		Na^+	
		out	center	out	center
ab initio	model	−90.4	−76.6	−64.2	13.8
MM	model	−65.2	−55.1	−47.8	57.7
	[1$_6$]starand	−69.8	−50.4	−55.0	65.7

[a] Ab initio data is obtained by MP2/6-31+G*//HF/6-31+G* (ref 11). Energies are in kcal/mol.

In the case of the model starand system, the molecular mechanics derived absolute binding energies are less favorable than those from ab initio calculations. Both methods, however, predict that central binding is disfavored in both Li^+ and Na^+ compared with outside binding. In the case of Na^+, the central binding energy is repulsive, presumably because the Na^+ ion is very large compared with the cavity size. Also, there is a large difference in binding energy between ab initio and molecular mechanics results for Na^+ for central binding. This large energy difference is not surprising considering the use of a rather hard van der Waals repulsive term and no electronic polarization induced in the molecular mechanical model. It is encouraging that the molecular mechanical method prefers outside binding for Li^+, just as the ab initio method does. The energy difference of the Li^+ complex between center and outside is 14 kcal/mol for ab initio and 10 kcal/mol for the force field method. The energy difference between Li^+ and Na^+ complexes for outer binding is 26 kcal/mol for ab initio and 17 kcal/mol for force field. Thus the force field seemingly may underestimate the absolute binding energy and the binding energy difference between the alkali metals.[17] When we compare the relative binding energy between the model and [1$_6$]starand, the starand is a slightly stronger host for alkali cations. The binding energy difference between Li^+ and Na^+ is 17 kcal/mol for the model and 15 kcal/mol for [1$_6$]starand.

In Table 4, the optimized distances of metal to oxygen (M−O) are compared with ab initio model starand data. The difference between ab initio and the force field model is less than 0.11 Å in each of the four cases, although the force field model predicts a slightly longer distance compared with ab initio distances. When we compare model and [1$_6$]starand, M−Os for [1$_6$]starand are slightly larger. The difference between [1$_6$]starand and model starand is about 0.03 Å in each of the five cases. Overall, the force field model gives reasonable results for both

(17) For binding energy evaluation, this level of theory seems appropriate. See: Hehre, W. J.; Yu, J.; Klunzinger, P. E. *A Guide to Molecular Mechanics and Molecular Orbital Calculations in SPARTAN*; Wavefunction, Inc.: CA, 1997; pp 47−48.

Table 4. Distances of Metal to Oxygen in Starand and Model Complexes[a]

		Li^+	Na^+	K^+	Rb^+	Cs^+
ab initio	model	1.904(1.883)	2.278(1.986)			
MM	model	1.988(1.917)	2.368(2.092)	2.702	2.829	3.033
	$[1_6]$starand	2.019	2.397	2.730	2.856	3.057

[a] Data in parentheses are for the unfavorable central binding. Ab initio data is obtained with 6-31+G* basis set (ref 11).

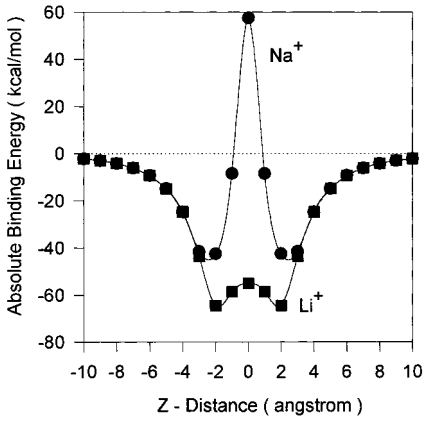

Figure 4. The binding energy with respect to distance from the center of mass along the principal axis.

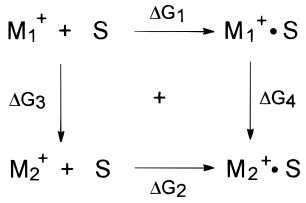

Figure 5. Thermodynamic cycle to obtain relative binding free energy.

geometries and energetics when we compare with ab initio and X-ray data.

Because the $[1_6]$starand has only one conformation, it is interesting to evaluate how the ion and ionophore interact as they approach each other. In Figure 4, the absolute binding energy of the model starand is plotted against the distance from the center of mass along the principal symmetry axis. Because the model system has a symmetric structure, the curves are symmetric with respect to distance. There is a strong peak for Na^+ and a small peak for Li^+ at the center. This indicates that Na^+ has strong steric interactions with the model system. In comparison, the curve for Li^+ also shows preference for outside binding, albeit in a much less drastic manner. Not surprisingly, the curves for Li^+ and Na^+ quickly become identical when the distances exceed 4 Å. There is about 2 kcal/mol of binding energy at a distance of 10 Å.

The thermodynamic cycle relevant to this study is shown in Figure 5. We are interested in the difference of free energy of complexation, ΔG_1 and ΔG_2 of M_1^+ and M_2^+ to the $[1_6]$starand. Although these values are difficult to calculate, ΔG_3 and ΔG_4, which involve perturbing metals from M_1^+ to M_2^+, are computationally feasible. Because the free energy is a state function, $\Delta\Delta G_{bind} = \Delta G_2 - \Delta G_1 = \Delta G_4 - \Delta G_3$. For simplicity, M^+•S will be used for a complex of an alkali ion and $[1_6]$starand hereafter; e.g., Li^+•S stands for the complex of lithium ion and $[1_6]$starand.

In all free energy perturbation simulations, the thermodynamic integration method was used. The SHAKE procedure[18] was employed to constrain all solute bonds bound to hydrogen atoms and all solvent bonds. A dielectric constant of 1.0 and a time step of 2.0 fs were used. For all simulations in aqueous solution, the TIP3P water model[19] was used together with periodic boundary conditions. These free energy simulation studies used a 10.0 Å cutoff and an NTP ensemble of 298 K and 1 atm with a coupling constant of 0.1 ps^{-1} for both temperature and pressure coupling. The solvent and solute were coupled to separate temperature baths. For the alkali cations, aqueous systems were constructed by immersing M^+ in a 22.4 Å cubic box containing 301 TIP3P waters and removing waters within 2.4 Å of the ion. Before starting free energy perturbation, the system was equilibrated for 10 ps, resulting in stable total energies. Each perturbation used 21 windows with 3 ps equilibration time and 3 ps of data collection time.

To generate the solvated host−guest systems, the minimized M^+•S system was placed in a rectangular flat box of TIP3P water, removing those within 2.4 Å of the solute and allowing 10 Å of solvent between the solute and the walls of the periodic box; this gave an initial box size of 35.8 × 35.8 × 27 $Å^3$ containing 888 solvent molecules.

Equilibrating this system for 10 ps resulted in solvated host−guest systems with very stable potential energy, indicating sufficient equilibration. Final coordinates and velocities for the equilibrated starand were used for the subsequent free energy calculations. During the initial Li^+ to Na^+ free energy perturbation, the ion drifted out of the starand. To prevent this from happening, a harmonic restraint of 1 kcal/mol/$Å^2$ was imposed on the three M−O(starand) distances as listed in Table 3. For example, the three equilibrium distances of Li^+•O was also perturbed from 2.019 to 2.397 Å when we perturb from Li^+•S to Na^+•S with coupling constant 0.05. The perturbations for other ions were performed similarly. The constraint energy was always very small compared with the potential energy. This kind of constraint has been successfully employed in FEP simulations of a host−guest system.[8] After the initial equilibration, Li^+ was perturbed into Na^+ over 21 windows with 1500 steps of equilibration and 1500 steps of data collection, resulting in a total simulation time of 63 ps. The final coordinates of this run were used as the starting point for the reverse perturbation from Na^+ to Li^+ for another 63 ps. Thus, we used a different trajectory for calculation of reverse simulations. The perturbations for the other ions were done similarly.

Results and Discussion

Gas-Phase Binding. We first calculated the relative binding energy differences for various alkali metals in the gas phase. These were done on the externally complexed structures (C_{3v}) because these are more stable than the corresponding internally complexed structures (D_{3d}). The calculations predict that the binding energy for Li^+ is −70 kcal/mol and that for Na^+ is −55 kcal/mol, thus giving a relative M^+•S binding enthalpy difference

(18) Ryckaert, J. P.; Ciccotti, G.; Berendesen, H. H. C. *J. Comput. Phys.* **1977**, *23*, 327.
(19) Jorgensen, W. L.; Chandrasekhar, J.; Madura, J. D. *J. Chem. Phys.* **1983**, *79*, 926.

Table 5. Relative Binding Enthalpies and Free Energies of M^+·S in the Gas Phase[a]

change	ΔE	ΔG_{for}	ΔG_{rev}	ΔG
$Li^+ \rightarrow Na^+$	14.84	14.74	14.65	14.69 ± 0.05
$Na^+ \rightarrow K^+$	9.59	9.32	9.22	9.27 ± 0.05
$K^+ \rightarrow Rb^+$	3.01	2.91	2.86	2.88 ± 0.02
$Rb^+ \rightarrow Cs^+$	4.28	4.06	4.08	4.07 ± 0.01

[a] ΔE is the relative binding energy, and ΔG is the relative binding free energy. Units are in kcal/mol.

Table 6. Relative ΔG of Hydration for the Perturbation of Alkali Ions in Water[a]

change	ΔG_{for}	ΔG_{rev}	ΔG_{sol}	Bayly[b]	Aqvist[c]
$Li^+ \rightarrow Na^+$	25.48	25.73	25.60 ± 0.13	25.6	23.7
$Na^+ \rightarrow K^+$	17.96	17.81	17.88 ± 0.07	17.3	17.6
$K^+ \rightarrow Rb^+$	5.62	5.57	5.59 ± 0.03	5.5	5.4
$Rb^+ \rightarrow Cs^+$	7.80	7.82	7.81 ± 0.01	7.9	7.8

[a] Energies are in kcal/mol. [b] Reference 9a. [c] Reference 14.

between Li^+ and Na^+ of 14.8 kcal/mol. These and the other ΔE values are shown in Table 5. This table shows that as the ionic radius becomes larger, the binding enthalpy becomes less favorable, which is reasonable because electrostatic effects are certainly the most important factor. We also performed the free energy perturbation of the system in the gas phase and determined a free energy difference between Li^+·S and Na^+·S of 14.74 kcal/mol, only 0.1 kcal/mol different from the enthalpy difference. Nevertheless, the free energy difference is smaller than the enthalpy difference, which implies that entropic contributions favor Na^+ binding more than Li^+. This is reasonable because as the ionic size gets larger, the ion sits farther away from the host, in turn allowing for more freedom of movement. The remaining data can be explained in the same manner. Despite the entropic element, however, the total binding free energy always shows preference for the smaller cations, a trend in accord with gas-phase experimental results involving other similar hosts.[6] Overall, the relative binding enthalpy predominantly governs the final relative binding free energy with minimal contribution from entropy.

When we consider the overall change from Li^+ to Cs^+, the enthalpy difference is 31.7 kcal/mol, and the binding free energy difference is 30.9 kcal/mol. Thus, the entropic contribution is only 0.8 kcal/mol. This entropy effect is small because the starand itself has only one conformation. In comparison, the entropy in 18-crown-6 arises mainly from its own conformational freedom and significantly affects the relative free energy.[6] Therefore, without substantial change in host conformation, the enthalpy difference can be a good approximation to the free energy difference in the gas phase.

Solvent Effect on Binding Free Energy. Because the [1$_6$]starand system has only one conformation without any single bond available to rotate, this system is free of the complexity involved in conformational changes of flexible hosts. The relative hydration free energies were obtained with the TIP3P water model, which gives accurate hydration free energies and reasonable radial distribution functions.[15] Table 6 contains the free energy data for various alkali metal ions in water. There are no substantial difference between our solvation energy values and previous results.

The results of free energy perturbation of M^+·S in aqueous solution are also listed in Table 7. The relative binding free energies are smaller than those of ions alone,

Table 7. Relative ΔG for the Perturbation of Alkali Ions Bound to Starand in Water[a]

perturbation	ΔG_{for}	ΔG_{rev}	ΔG_{sol}	ΔG_b
$Li^+ \rightarrow Na^+$	21.85	21.69	21.77 ± 0.08	−3.83
$Na^+ \rightarrow K^+$	16.77	16.71	16.74 ± 0.03	−1.14
$K^+ \rightarrow Rb^+$	5.25	5.29	5.27 ± 0.02	−0.32
$Rb^+ \rightarrow Cs^+$	7.59	7.64	7.62 ± 0.03	−0.20

[a] Energies are in kcal/mol.

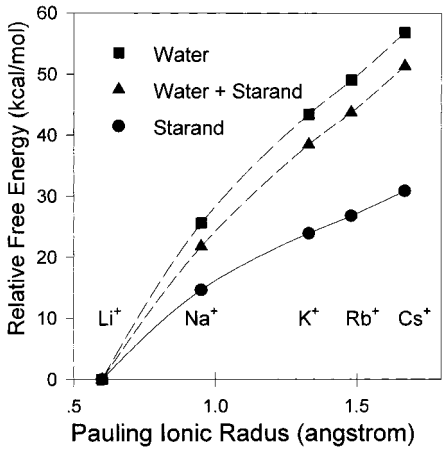

Figure 6. The relative stabilities of alkali metal ions in various environments.

thus leading to negative relative binding free energies. In Figure 6, the relative free energies of the five alkali ions in three different conditions are plotted relative to the value for Li^+. In this figure, ● symbolizes the relative binding energies of M^+·S complexes in the gas phase (without water), ■ denotes the free energies of M^+ in water (without starand), and ▲ represents the M^+·S complexes in aqueous solution (with both starand and water). It is reasonable for the ▲ points to fall between ● and ■, because they are affected by both water and starand. Evidently, the effect of water outweighs the binding to a [1$_6$]starand, as can be seen by how ▲ lies closer to ■ than ●. Furthermore, as the ionic radius gets larger, ▲ gets much farther from ●. As the ionic radius gets larger, the ion dwells farther away from the starand while feeling more water solvent exposure. For example, a greater portion of the Cs^+ surface area in Cs^+·S is accessible to water solvent compared to that of the Li^+ surface area in Li^+·S.

Coordination numbers often provide useful information regarding the level of solvation, so we examined these values to use if the larger ions in the complexes are better solvated. To determine the coordination numbers, we performed radial distribution function (RDF) analyses, using simulation conditions identical to those in FEP. A harmonic restraint of 1 kcal/mol/Å^2 to the three M−Os was also employed, and the equilibrium distance for the restraints was based on optimized M^+−O distance data in the gas phase. Each system was equilibrated for 25 ps with this restraint before the collection of RDF data for 100 ps.

The RDF plots of M^+−O(water) in bare ions and those in M^+·S are compared in Figure 7. The peak heights for bare ions (A) are substantially higher than the corresponding peaks for M^+·S (B). For bare ions, the position of the peak shifts to the right as the ionic radius increases, while the peak height varies inversely with the ionic radius. For M^+·S, the trends are basically the

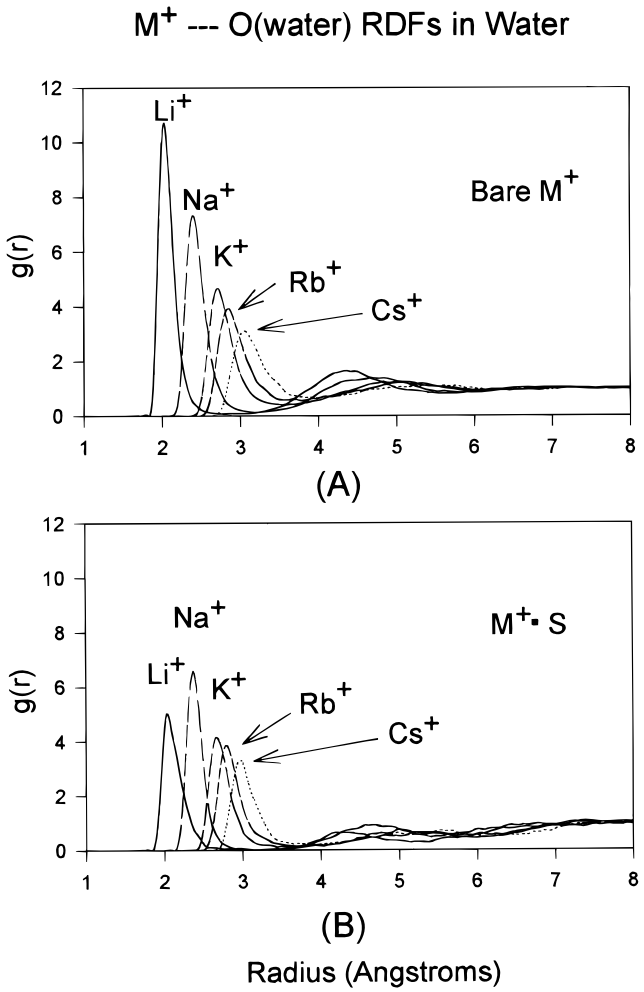

Figure 7. Comparison of RDFs of M^+−O(water) between bare M^+ and M^+•S in aqueous solutions; (A) bare ions and (B) their [1_6]starand complexes.

same as for the bare ions, except that the peak height of Li^+ is lower than that of Na^+. Why is the peak height of Li^+ lower than that of Na^+ for M^+•S, whereas the reverse is true for bare ions? To understand this, we focused our attention on the ion and the three coordinated ligand oxygens. The angle between the principal axis and M^+−O direction is drawn in Figure 8. As the radius increases, the M^+−O distance gets longer and angle (α) and height (**H**) get larger. The angle α for Li^+ is very small compared with angles for other ions (119° vs 133−145°). The height **H** for Li^+ is also very small compared with those for other ions (1.0 Å vs 1.6−2.5 Å). It would be more unfavorable for water oxygens to coordinate with Li^+ than with Na^+, because the O(water)−O(starand) distances would be significantly closer. It seems that Li^+ is somewhat shielded by the three coordinated host oxygen atoms by small values of α, **H**, and a small ionic radius. Overall, the exceptionally small size of Li^+ ends up creating an environment that is less compatible with waters coordinated to Li^+ of Li^+•S.

One may be tempted to explain the relative binding free energies of M^+•S in water as the number of waters "displaced" upon binding. Because this number ($N_M - N_C$ in Table 8) appears largest for Rb^+ and Cs^+, it is not simply the difference in coordination number. Free energy cost of displacing a water is larger when the ion is smaller. Thus, the trend in aqueous free energies can

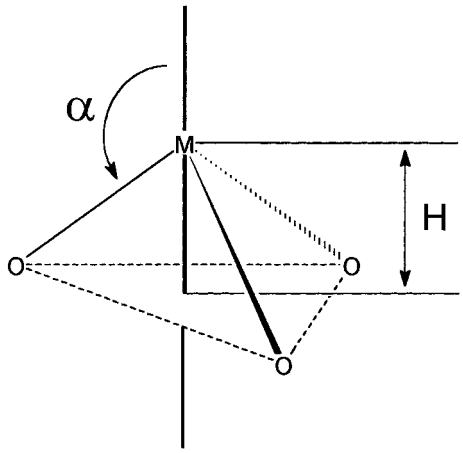

	Li	Na	K	Rb	Cs
α	119.4	132.8	139.9	142.0	144.9
H	0.99	1.63	2.09	2.25	2.50

Figure 8. Schematic drawing to show that Li^+ is shielded by three coordinated oxygen atoms of [1_6]starand. Here, α is the angle between the principal axis and the direction of M^+−O; **H** is the distance from the plane of the three oxygen atoms to the alkali ion.

Table 8. Ion−Water Oxygen RDF Peaks and Coordination Numbers for Alkali Metal Ions in Aquous Solutions[a]

	alkali metal only					
	peak				M^+•S	
ion	this work	Aqvist	expt	N_M	peak	N_C
Li^+	2.04	2.03	2.00∼2.08	4.48	2.04	2.51
Na^+	2.40	2.39	2.35∼2.42	5.60	2.37	3.70
K^+	2.72	2.75	2.73∼2.80	6.37	2.67	4.17
Rb^+	2.85	2.89	2.88	7.59	2.80	4.68
Cs^+	3.06	3.10	3.09∼3.15	8.34	2.97	5.04

[a] N_C is denoted for the water−oxygen coordination numbers of complexes, and N_M for those of metal ions.

be simply that the less the free energy cost for desolvating the ion, the stronger is the binding.

Absolute Binding Free Energy. So far, we have studied the relative binding free energies of various alkali metals in water. However, it is also of great interest to see how large their absolute binding free energies are. To do this, we calculated the absolute free energy of hydration, using electrostatic decoupling methods. For example, Rb^+ was first perturbed into Rb^0, which has no charge; this Rb^0 is then perturbed into Du^0, which has no volume. Because we are perturbing metal ions to nothing, we need to correct two things compared with previous van der Waals parameter perturbation. Because the charge of the metal ion changes during the perturbation and we use a cutoff, the electrostatic effect should be corrected. We did this by the Born formula: $\Delta G_{corr} = -166z^2/r_{cut}$ where z is the charge of the ion and r_{cut} is the cutoff radius. Because the ions are vanishing, the harmonic restraint effects imposed to keep the metal ion from decomplexation should be corrected in the complexes. We corrected this effect by extrapolation, varying the restraint value from 1.0, 0.3, and 0.1 kcal/mol × $Å^{-2}$.

Table 9. Absolute Δ*G* for the Perturbation of Alkali Ions to Dummy in Water[a]

perturbation	ΔG_{for}	ΔG_{rev}	ΔG_{ave}	ΔG_{sol}[b]
		M^+		
$Rb^+ \rightarrow Rb^0$	68.24	69.38	68.81 ± 0.57	
$Rb^0 \rightarrow Du^0$	−6.09	−5.74	−5.92 ± 0.19	−83.64
$Cs^+ \rightarrow Cs^0$	61.48	61.76	61.62 ± 0.14	
$Cs^0 \rightarrow Du^0$	−7.35	−6.91	−7.13 ± 0.22	−75.24
		M^+·S		
$f_{rest} = 1.0$				
$Rb^+ \rightarrow Rb^0$	70.68	69.54	70.11 ± 0.57	
$Rb^0 \rightarrow Du^0$	−9.98	−10.50	−10.24 ± 0.26	−80.62
$Cs^+ \rightarrow Cs^0$	64.61	64.71	64.66 ± 0.05	
$Cs^0 \rightarrow Du^0$	−11.85	−11.51	−11.68 ± 0.17	−73.73
$f_{rest} = 0.3$				
$Rb^+ \rightarrow Rb^0$	70.37	69.45	69.91 ± 0.46	
$Rb^0 \rightarrow Du^0$	−8.88	−9.07	−8.97 ± 0.10	−81.69
$Cs^+ \rightarrow Cs^0$	64.30	64.52	64.41 ± 0.11	
$Cs^0 \rightarrow Du^0$	−10.11	−10.45	−10.28 ± 0.17	−74.88
$f_{rest} = 0.1$				
$Rb^+ \rightarrow Rb^0$	69.15	69.54	69.35 ± 0.19	
$Rb^0 \rightarrow Du^0$	−7.72	−8.33	−8.02 ± 0.30	−82.07
$Cs^+ \rightarrow Cs^0$	63.50	63.68	63.59 ± 0.09	
$Cs^0 \rightarrow Du^0$	−9.55	−8.79	−9.17 ± 0.38	−75.17

[a] Energies are in kcal/mol. Rb^0 and Cs^0 are denoted for neutral alkali metals, Du^0 for dummy atom. [b] Born energy corrected free energies of solvation ($Du^0 \rightarrow M^+$). The energies are corrected by $\Delta G_{corr} = -166z^2/r_{Born}$ where z is the charge of the ion and r_{Born} is the cutoff radius; f_{rest} is harmonic restraints between metal ion and coordinated oxygen atoms (kcal mol^{-1} $Å^{-2}$).

During this perturbation, the same protocol as in the relative free energy calculation, including constants on the ion in the complex, were used.

In Table 9, the absolute solvation energies are listed for metal ions and their complexes. An 8 Å cutoff was used, which not surprisingly led to an underestimate of the absolute solvation energies (ΔG_{sol}) for Rb^+ and Cs^+. As has been found before for periodic boundary conditions, using a simple Born correction leads to an overestimate of the magnitude of ΔG_{sol}. The calculated ΔG_{sol} values of −83.7 (Rb^+) and −75.3 (Cs^+) kcal/mol are larger than the values of −75.5 (Rb^+) and −67.8 (Cs^+) kcal/mol from experiments.[20] Nontheless, the difference of solvation free energy in simulation (8.4 kcal/mol) is comparable to that in experiment (7.7 kcal/mol).

For complexes, we calculated the absolute solvation free energies for the various harmonic restraints (f_{rest}). As the restraint gets smaller, the magnitude of solvation energy becomes larger. Extrapolation gives absolute solvation energies of −82.20 kcal/mol for Rb^+ and −75.35 kcal/mol for Cs^+ at the extreme value of no restraints (i.e., $f_{rest} = 0$).

The absolute free energies of the ions in M^+·S are smaller than or comparable to those of bare ions. For example, the hydration energy of Rb^+ is −83.6 kcal/mol, compared to −82.2 kcal/mol in Rb^+·S. Therefore the binding energy in water becomes +1.4 kcal/mol for Rb^+ and −0.1 kcal/mol for Cs^+. Because the binding free energies are either positive or close to zero, the ions will not bind tightly to the [1_6]starand. This was a somewhat unexpected result in view of the previous ab initio calculations, which showed that the [1_6]starand model had a slightly higher affinity toward alkali cations than 12-crown-4.[21] Even though the absolute free energies are less accurate than the relative ones, it appears clear that the [1_6]starand is not strong host for the various alkali metal ions.

Summary

One of the most difficult problems in theoretical simulations of host−guest chemistry is the insufficient sampling involving host and guest conformations. Because [1_6]starand exhibits a very rigid structure with only a single conformation available, insufficient sampling should not confound the simulations. By comparing with X-ray and ab initio data, we also showed the force field parameters give rise to good structures and energetics for the alkali metal and starand system, at least qualitatively. After validating the force field accuracy without encountering any problems related to conformations, our next step was to predict the relative binding free energies in water. This attempt at prediction was also motivated by other recent successful simulations using FEP methods. By comparing the energy and the free energy of binding in the gas phase, we demonstrated that the entropy effect is in fact small for this system, contrary to the conformational variation that is the major entropic contribution in flexible hosts. The order of stability of M^+·S in the gas phase is Li^+·S > Na^+·S > K^+·S > Rb^+·S > Cs^+·S. This order turns around completely in water, giving Li^+·S < Na^+·S < K^+·S < Rb^+·S < Cs^+·S. The absolute binding energy calculations predicted that the [1_6]starand does not bind strongly to alkali ions in water. Overall, the starands including [1_6]starand do not seem to possess as strong an affinity toward alkali metal ions in water as one might expect from their structures.

Acknowledgment. Seung Joo Cho thanks the KRF for financial support and Dr. Elaine C. Meng for sharing the MINMD program. P.A.K. thanks the NSF for support through CHE94-17458.

JO982367G

(20) (a) Marcus, Y. *Ion Solvation*; Wiley & Sons: New York, 1985. (b) Burgess, M. A. *Metal Ions in Solution*; Ellis Horwood Ltd.: England, 1978.

(21) The ab initio calculation was done by MP2/6-31+G*//HF/6-31+G*. The binding energies of Li^+·S and Na^+·S are 90 and 64 kcal/mol, respectively. Those of 12-crown-4 complexes are 89 and 63 kcal/mol, respectively.